A Direct Synthesis of Mesoporous Carbons with Bicontinuous Pore Morphology from Crude Plant Material by Hydrothermal Carbonization

Maria M. Titirici,[†] Arne Thomas,[†] Shu-Hong Yu,[‡] Jens-O. Müller,[§] and Markus Antonietti*,[†]

Department of Colloid Chemistry, Max Planck Institute of Colloids and Interfaces, Am Muehlenberg 1, D-14476 Potsdam, Germany, Division of Nanomaterials and Chemistry, Hefei National Laboratory for Physical Sciences at Microscale, Structure Research Laboratory of CAS, Department of Materials Science and Engineering, University of Science and Technology of China, Hefei 230026, P. R. China, Department of Inorganic Chemistry, Fritz Haber Institute of the Max Planck Society, Faradayweg 4-6, D-14195 Berlin, Germany

Received March 16, 2007. Revised Manuscript Received June 14, 2007

Hydrothermal carbonization is a convenient way to convert biomass at rather moderate conditions into carbonaceous nanostructures, here, mesoporous network structures. A structural view on the micro- and nanoscale reveals interesting features defining the usefulness and application possibilities of the resulting carbonaceous materials as supports and for sorption purposes. Whereas weakly connected plant tissues result in good yields of carbon nanoparticles with very small sizes where the porosity is mainly interstitial, "hard" plant tissue is structurally transformed into a carbon replica with a rather well-defined, bicontinuous mesopore structure.

Introduction

The search for meaningful ways to transfer biomass into useful materials, more efficient energy carriers, and/or carbon storage deposits is a key question of our days. Transfer of biomass toward carbon-rich material with potential megascale application is an option to sequester carbon from plant material, taking it out of the short-term carbon cycle and therefore binding CO_2 efficiently and in an even useful way. Coalification of biomass is a natural chemical process, but takes place on the time scale of some hundred (peat) to millions (black coal) of years. Because of its slowness, it is usually not considered in material synthesis or bioenergy exploitation schemes.

There are countless trials in the literature to replicate carbon formation from carbohydrates with faster chemical processes, and hydrothermal carbonization (HTC) seems to be especially promising. Early experiments were carried out by Bergius and Specht, who described in 1913 the hydrothermal transformation of cellulose into coallike products.[1] In 1932, more systematic investigations were performed by Berl and Schmidt, who varied the source of biomass and treated the different samples in the presence of water at temperatures between 150 and 350 °C.[2] The latter authors also summarized in a series of papers in 1932 the knowledge about the emergence of coal of those days (e.g., ref 3). Later, Schuhmacher, Huntjens, and van Krevelen analyzed the influence of pH on the outcome of reaction and found large differences in the decomposition schemes, basing their statements, however, mainly on C/H/O elemental composition analysis.[4] The described accelerations of coalification by a factor of 1×10^6 to 1×10^9 under rather soft conditions make hydrothermal carbonization (HTC) a considerable technical alternative for carbon generation for larger scales, either for sequestering carbon from biomass or for the technical synthesis of carbon nanomaterials.

A key observation of controlled carbon structure synthesis was reported with the low temperature (≤200 °C) hydrothermal synthesis of carbon microspheres using sugar or glucose as precursors.[5,6] Recently, our group has found that the presence of metal ions can effectively accelerate hydrothermal carbonization of starch, which shortens the reaction time to some hours but also directs the synthesis toward various metal/carbon nanoarchitectures such as Ag@Carbon nanocables,[7] carbon nanofibers,[8] and spheres.[7] Iron ions and iron oxide nanoparticles were shown to effectively catalyze the hydrothermal carbonization of starch and rice grains under very mild conditions (≤200 °C) and have a significant influence on the morphology of the formed carbon nano-

* Corresponding author. E-mail: pape@mpikg-golm.mpg.de. Fax: 49 331 567 9502.
[†] Max Planck Institute of Colloids and Interfaces.
[‡] University of Science and Technology of China.
[§] Fritz Haber Institute of the Max Planck Society.

(1) Bergius, F. *Die Anwendung hoher Drucke bei chemischen Vorgängen und eine Nachbildung des Entstehungsprozesses der Steinkohle*; Verlag Wilhelm Knapp: Halle an der Saale, Germany, 1913; p 58.
(2) Berl, E.; Schmidt, A. *Liebigs Annalen Chemie* **1932**, *493*, 97−123.
(3) Berl, E.; Schmidt, A.; Koch, H. *Angew. Chem.* **1932**, *45*, 0517−0519.
(4) Schuhmacher, J. P.; Huntjens, F. J.; Vankrevelen, D. W. *Fuel* **1960**, *39* (3), 223−234.
(5) Sun, X. M.; Li, Y. D. *Angew. Chem., Int. Ed.* **2004**, *43* (5), 597−601.
(6) Wang, Q.; Li, H.; Chen, L. Q.; Huang, X. J. *Carbon* **2001**, *39* (14), 2211−2214.
(7) Yu, S. H.; Cui, X. J.; Li, L. L.; Li, K.; Yu, B.; Antonietti, M.; Cölfen, H. *Adv. Mater.* **2004**, *16* (18), 1636−1640.
(8) Qian, H. S.; Yu, S. H.; Luo, L. B.; Gong, J. Y.; Fei, L. F.; Liu, X. M. *Chem. Mater.* **2006**, *18* (8), 2102−2108.

10.1021/cm0707408 CCC: $37.00
Published on Web 07/28/2007

materials In the presence of Fe^{2+} ions, both hollow and massive carbon microspheres can be obtained. In contrast, the presence of Fe_2O_3 nanoparticles leads to very fine, ropelike carbon nanostructures,[9] which indicates that those solution processes share common features with the gas-phase synthesis of carbon nanostructures.

From an energetical point of view, HTC is—contrary to the standard high-temperature carbonization reactions—an exothermic process and even liberates about a third of the combustion energy of the sugars throughout dehydration while forming the condensed carbons (because of the high thermodynamic stability of water). Besides being fast and simple, HTC also inherently requires wet starting products/biomass, as effective dehydration occurs only in the presence of water. In addition, the final carbon can be easily filtered off the reaction solution. This way, complicated drying schemes and costly isolation procedures can conceptually be avoided. The carbon efficiency of HTC is close to 1, i.e., practically all of the starting carbon stays bound in the final carbonaceous material. Carbon structures produced like that, either for energy or materials use, are therefore at least energy- and CO_2-neutral. Low-tech biomass processing to hydrophilic porous carbon structures might therefore represent one of the few existing, efficient carbon sinks that can be technologically accessed to handle significant parts of the CO_2 problem.[10]

It is therefore the purpose of the present contribution to extend HTC from complex biomass to the convenient synthesis of mesoporous carbonaceous materials. This is a highly appealing target: in the past decade, considerable efforts have been directed toward the synthesis of mesoporous carbons with controlled mesopore structure.[11,12] The property combination of high surface area, narrow pore size distributions, and regular frameworks of mesoporous materials with the unparalleled chemical, mechanical and thermal stability of carbonaceous substances makes mesoporous carbons interesting candidates for several applications such as catalysis, sorption, and electrode materials. With very few recent significant exceptions,[13,14] the synthesis of mesoporous ordered carbon generally relies on the method developed by Ryoo et al.,[15] where a high-temperature carbonization is performed inside ordered mesoporous silica templates, followed by subsequent removal of the silica matrix. The first ordered mesoporous carbon replica called CMK-3 was obtained using SBA-15 as silica template.[16] These structures have enabled us to reveal the superior potential of mesoporous carbons in a variety of areas, but it stays obvious that alternative synthetic approaches toward such structures have to be found when technical questions and large-scale, low-price applications are to be addressed. Such applications for mesoporous carbons include their use as sorption coal for drinking water purification or as a water and ion-binding conditioner to improve soil quality. For that, the carbon material, however, not only has to be highly porous but also equipped with chemical functionality, i.e., it must be water-wettable and has to contain appropriate functional ion-binding groups along its surface.

It will be shown that complex, hydrothermally carbonized waste biomass can be directed to such complex structural motifs under simultaneous control of surface polarity. We specifically selected starting products regarded as "waste biomass," which are known to be hard to use otherwise, and applied different HTC conditions. The specific starting products (sugar beet chips, pine cones, pine needles, oak leafs, and orange peels) are known to contain, besides cellulose and hemicelluloses, up to 35% lignins, together with smaller amounts of terpenes, oils and waxes (pine needles), tannins and polyphenols (oak leaves), and flavones and limonenes (orange peels). These additional substances usually hinder microbial degradation of the respective biomass, but are in HTC a source of potentially useful chemical surface functionality. It is examined if and how these additional components interfere with the HTC of the majority component (polysaccharides). The composition as well as the nanostructure and porosity of the resulting carbonaceous materials are analyzed by Raman spectroscopy, wide-angle X-ray diffraction, gas sorption analysis, transmission electron microscopy (TEM), X-ray photoelectron spectroscopy (XPS), and high-resolution scanning electron microscopy (HRSEM).

Experimental Section

Pine needles, pine cones, and oak leaves were picked from the author's garden and used as received. Orange peels were provided by our cantina. Citric acid was obtained from Aldrich Co. and used as received. Sugar beet chips, depleted of sugar, were provided by BMA Co.

The reaction was carried out in a nonstirred, 60 mL capacity Teflon-lined stainless steel autoclave, which was put in a programmable oven. In a typical procedure, 5−20 g of biomass was dispersed in 40 mL of deionized water. Ten milligrams of citric acid was added to ensure comparable acidic carbonization conditions. The autoclave was sealed and tempered at 180−250 °C (default 200 °C) for 16 h and then allowed to cool to room temperature. The products were filtered off, washed several times with distilled water and absolute ethanol, and finally dried in a vacuum at 60 °C for 4 h.

Warning: *we seriously caution against repeating the experiments without additional safety measures using too high concentrations of too easily carbonizable material, as the reaction is exothermic.* This was already pointed out in the early review of Bergius.[17] Although it is only water and carbohydrate, up to 30% of the heat of combustion is liberated, making spontaneous breakouts of the reaction rather violent.

The products were characterized by a Leo 912 Omega electron microscope operating at 120 kV. Raman spectra were recorded at

(9) Cui, X. J.; Antonietti, M.; Yu, S. H. *Small* **2006**, *2* (6), 756−759.
(10) About 8% of the estimated terrestrial biomass growth would be sufficien to bind the complete current yearly CO_2 production from oil (4 km^3). This is less than the overall agricutlural biomass waste.
(11) Ryoo, R.; Joo, S. H.; Kruk, M.; Jaroniec, M. *Adv. Mater.* **2001**, *13* (9), 677−681.
(12) Lu, A. H.; Kiefer, A.; Schmidt, W.; Schüth, F. *Chem. Mater.* **2004**, *16* (1), 100−103.
(13) Meng, Y.; Gu, D.; Zhang, F. Q.; Shi, Y. F.; Yang, H. F.; Li, Z.; Yu, C. Z.; Tu, B.; Zhao, D. Y. *Angew. Chem., Int. Ed.* **2005**, *44* (43), 7053−7059.
(14) Kosonen, H.; Valkama, S.; Nykanen, A.; Toivanen, M.; ten Brinke, G.; Ruokolainen, J.; Ikkala, O. *Adv. Mater.* **2006**, *18* (2), 201.
(15) Ryoo, R.; Joo, S. H.; Jun, S. *J. Phys. Chem. B* **1999**, *103* (37), 7743−7746.
(16) Jun, S.; Joo, S. H.; Ryoo, R.; Kruk, M.; Jaroniec, M.; Liu, Z.; Ohsuna, T.; Terasaki, O. *J. Am. Chem. Soc.* **2000**, *122* (43), 10712−10713.
(17) Bergius, F. *Naturwissenschaften* **1928**, *16* (1), 1−10.

room temperature with a LABRAM-HR Confocal Laser MicroRaman Spectrometer. FT-IR spectra were recorded using a Varian 600 FT-IR Spectrometer (primary wavelength 532 nm). Highly resolved scanning electron microscopy (HRSEM) was performed on a Zeiss DSM 940 A. Nitrogen adsorption−desorption isotherms were measured at 77 K with a Micromeritics Tristar 3000 system. High-resolution transmission electron microscopy (HRTEM) and electron energy-loss spectroscopy (EELS) were performed in a Philips TEM/STEM CM 200 FEG transmission electron microscope equipped with a field-emission gun and a GATAN Tridiem imaging filter. The acceleration voltage was set to 200 kV. X-ray photoelectron spectroscopy (XPS) measurements were taken on a Physical Electronics ESCA 5600 spectrometer with a monochromatic Al−K_α X-ray source at a power of 200 W/14 kV and a multichannel detector OmniIV. The electron takeoff angle (θ) to the sample surface was adjusted to 45°. Spectra were obtained for both high-resolution mode (pass energy of 58.70 eV) for C1s, O1s, and Sn3d and low-resolution mode (pass energy of 187.85 eV). Binding energies for the high-resolution spectra were calibrated by setting C1s at 284.6 eV.

Results and Discussion

The different biomass compounds were heated in closed autoclaves in the presence of an acidic catalyst (citric acid) to various temperatures for 16 h. Samples treated below 180 °C showed only weak or no conversions for cellulose-containing species; temperatures exceeding 220 °C can result in a runaway of the reaction, with reactions at 250 °C sometimes tending to generate heat and pressure, which burst the safety plate of the autoclave. The current systematic work was therefore restricted to a temperature of 200 °C.

All the reactions at those low temperatures under acidic conditions are characterized by no or only weak pressure buildup; that is, decomposition of the different biomass into CO_2 or methane plays only a minor role. This is interesting to note, as the classical experiments by Bergius at higher temperatures and neutral or alkaline conditions always gave a significant fraction of CO_2,[12] which finally turns into the predominant product in supercritical hydrothermal gasification at 600 °C and 250 bar under alkaline conditions.[18] We attribute the suppression of gas formation to a more controlled decomposition scheme under acidic conditions that is shifted to dehydration reactions and coalification instead of hydrid transfer and decarboxylation.

Spectroscopically and by elemental analysis, all hydrothermal carbons, even from complex biomass, are very similar to peat or vitrinites. Raman spectroscopy (Figure 1) shows the typical in-plane vibrations of only structurally connected carbon, as they are very typical for activated, amorphous carbons. IR spectroscopy (Figure 2) reveals the signatures of functional groups, which point to a very polar surface structure of the hydrothermal carbons, such as phenolic residues, carbonyl and hydroxyl functions, and aliphatic double bonds.

As compared to mineral coals, the amount of carboxylic acid groups is rather low, underlining the highly reductive conditions throughout the hydrothermal, oxygen-free carbonization reaction (the constituting aldoses transfer into aldehydes onto the surface). Also, the C/H/O ratios are also not surprising and move along composition lines previously identified in HTC experiments on cellulose,[5] i.e., C/O ratios of about 4−6 and H/C ratios of about 0.70. The findings are also very similar to HTC of the molecularly soluble glucose and starch.[7,9] In IR spectroscopy, pine needles and orange peels show the strongest hydrocarbon bands corresponding to their original oil and terpene content. The fact that these compounds are partially bound to the dehydrated carbon scaffold is supported by appearance of the products: the resulting carbon (e.g., from orange peels) just weakly smells and has no bitter taste. Extraction with chloroform gives a tarlike fraction, the spectra of which are typical for tannins and phenols.

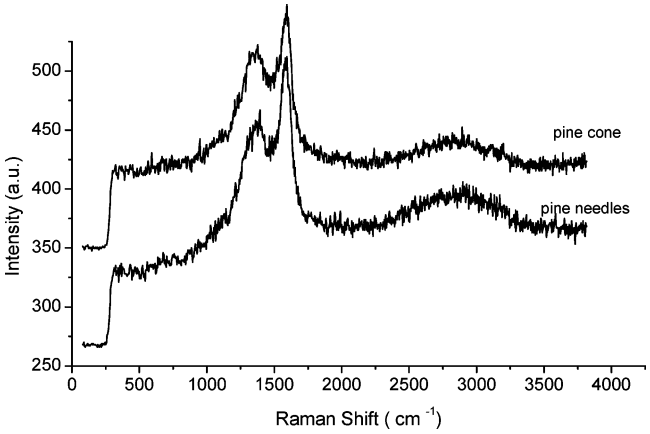

Figure 1. Raman spectra of two porous carbonaceous materials made from biomass.

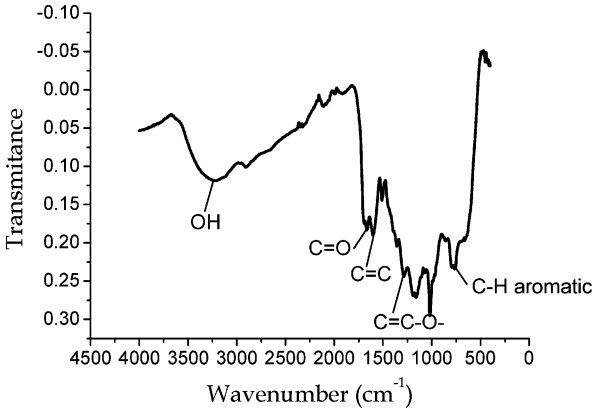

Figure 2. Typical IR spectrum of hydrothermal carbon, characterizing the accessible surface functionalities within the structure.

XPS data can support the IR data and reveal the local binding situation of both carbon and oxygen units (Figure 3).

The XPS data indicate that the structural carbon is in majority in a sp^2-binding situation. The C1s peak shows a very broad feature due to the disorder in the material. Carbon functionalities include C═O, C−OH, and C−H. However, the detailed fitting of the different groups is not unambiguous because of the charging of the material and the broadening of the feature at 284.6 eV, leading to the contribution at 283.5 eV. Similarly, the fitting of the O1s spectrum is not straightforward either, as chemical shifts due to C═O and C−OH groups cannot be clearly separated from the contributions from adsorbed H_2O. Further work is in progress to

(18) Schmieder, H.; Abeln, J.; Boukis, N.; Dinjus, E.; Kruse, A.; Kluth, M.; Petrich, G.; Sadri, E.; Schacht, M. *J. Supercrit. Fluids* **2000**, *17* (2), 145−153.

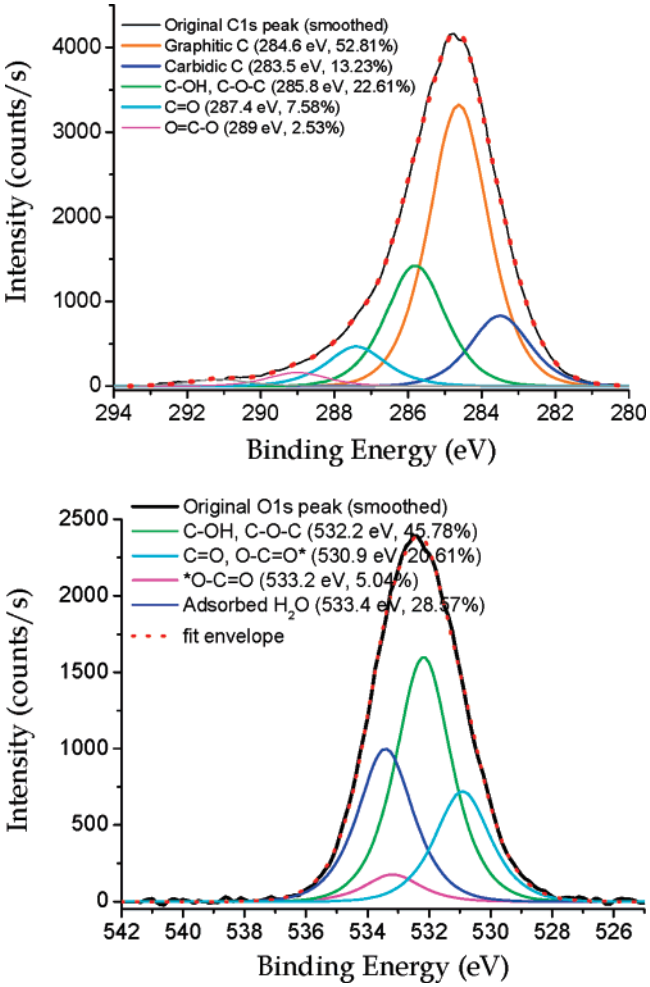

Figure 3. XPS data of carbonized sugar beet chips: (a) carbon edge; (b) oxygen edge.

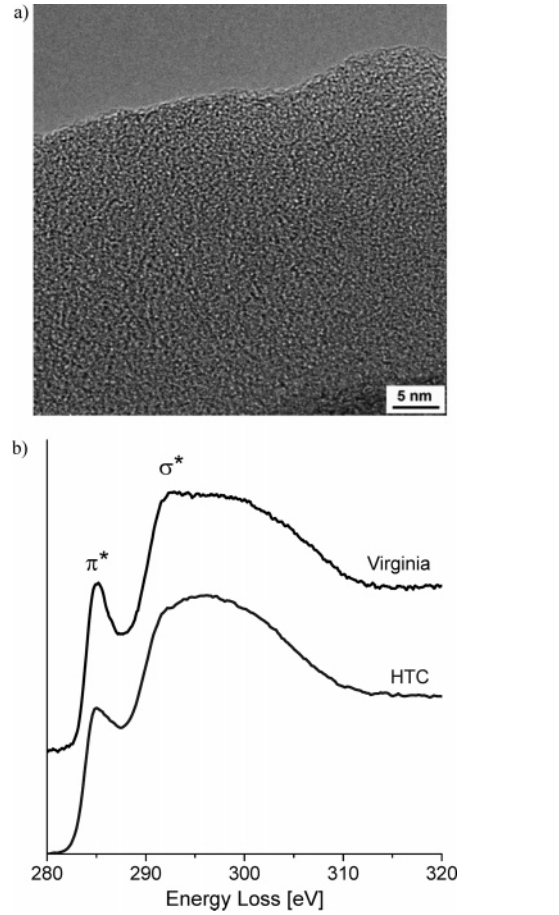

Figure 4. (a) HRTEM image of carbon from HTC illustrating the high disorder in the material; (b) EELS spectra of Virginia coal and carbon from HTC, showing clear dissimilarities in the ELNES.

enhance the information about the local carbonization structures from XPS work. However, the data again support the model of a nonoxidative transformation in the hydrothermal process and the absence of hydrogen shift reactions.

HRTEM and EELS measurements were performed in order to reveal further details about the microstructure, morphology, and electronic structure. HRTEM shows that the material from HTC essentially consists of disordered carbon. The projection of the surface of the particles does not reveal any ordering in graphene layers either (Figure 4a). This is confirmed by measuring the carbon-K-ionization edge by EELS. The spectra given in Figure 4b are dominated by two features. Transitions from 1s to π^* states are giving the main signal at 285 eV, whereas the signal at energy losses >290 eV mainly represents transitions from 1s to σ^* states.[19] The spectrum from the HTC carbon shows a distinct difference in the ELNES compared to Virginia anthracitic coal. The π^* peak in the EELS spectrum from the carbonization material is weaker in comparison to the one from coal. Additionally, the peak at 292 eV clearly distinguishable in the spectrum from coal is not as prominent in the case of HTC carbon. This variation in the spectra validates the conclusion from HRTEM, the higher level of disorder. Extended aromatic or graphitic layered systems are apparently not present. The intensity at 286−288 eV varies with the amount of functionalities or heteroatoms in the samples.[20−22] This feature is more prominent in the case of carbon from HTC, in agreement with XPS measurements.

The major difference of the present experiments to the decomposition of pure, simple carbohydrates is not found on the molecular scale, but was identified in the structural analysis in the micrometer and upper nanometer range, revealing essentially two structural decomposition pathways for the complex biomass. Under the applied conditions (16 h and 200 °C), all mechanically soft biomass without extended crystalline cellulose scaffold (orange peels, pine needles) was essentially disintegrated and liquefied, resulting in a dispersion of carbon nanoparticles as a majority fraction of the product. SEM images (Figure 5), here for the pine needles, supports that the original texture is dissolved, i.e., hydrolyzed and carbonized.

Instead, a very fine powder comprising 20−200 nm sized globular carbonaceous nanoparticles is found. The dropletlike appearance of these structures indicate that, similar to the hydrothermal decomposition of glucose, the process progresses

(19) Egerton, R. F. *Electron Energy-Loss Spectroscopy in the Electron Microscope*, 2nd ed.; Plenum Press: New York, 1996; p 485.

(20) Varlot, K.; Martin, J. M.; Gonbeau, D.; Quet, C. *Polymer* **1999**, *40* (20), 5691.

(21) Jäger, C.; Henning, T.; Schlögl, R.; Spillecke, O. *J. Non-Cryst. Solids* **1999**, *258*, (1−3), 161−179.

(22) Müller, J. O.; Su, D. S.; Jentoft, R. E.; Wild, U.; Schlögl, R. *Environ. Sci. Ecol.* **2006**, *40* (4), 1231−1236.

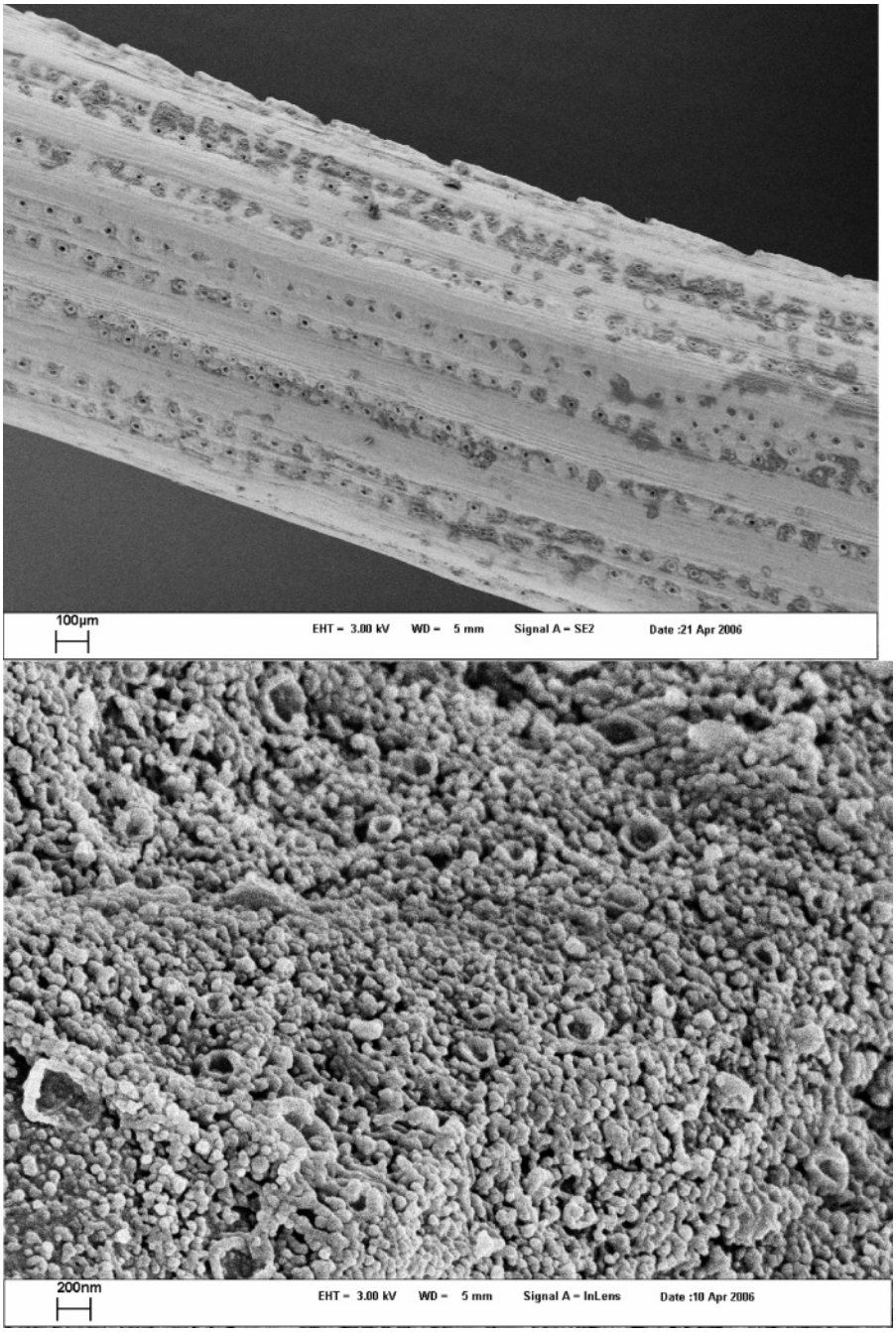

Figure 5. HRSEM of pine needles (a) before and (b) after being hydrothermally carbonized at 200 °C for 12 h. Upper scale bar, 100 μm; lower scale bar, 200 nm. The original tissue texture is disintegrated. Instead, an aggregate composed of 20−200 nm carbonaceous nanoparticles is obtained.

via liquid intermediates, which then later polymerize/cyclize to the final coal-like material. GC-MS data on products gained after 2 h support older observations[23,24] that for the polymeric carbohydrates, the decomposition essentially progresses via the hydroxymethyl furfural route. It is interesting to note that, very similar to the hydrothermal dehydration of starch, both the remainders of dense globules as well as hollow spheres can be observed (the latter as "deflated" spheres in Figure 5b). Contrary to glucose or pure starch, the nanoparticles are, however, in general much smaller for the complex biomass as a starting product. This increase in particle number might be due to an improved particle nucleation by nanoscopic side products formed by nondegradable secondary components (salts, polyphenoles, tannins, carboxylic acids), as known from classical emulsion polymerization. On the other hand, the coupled increase in surface area is beneficial for the desired materials applications, i.e., water and ion binding as well as capillarity. Because of the decomposition and the presence of other polar components in the biomass, the surface chemistry of the carbon nanospheres is as such that they are highly hydrophilic and easily water-dispersable. Both aspects, globular nanostructure and hydrophilic surface chemistry, are already attractive for a number of materials applications, e.g., some of those where usually polymer latexes are applied.

(23) Asghari, F. S.; Yoshida, H. *Ind. Eng. Chem. Res.* **2006**, *45* (7), 2163−2173.
(24) Bobleter, O. *Progr. Polym. Sci.* **1994**, *19* (5), 797−841.

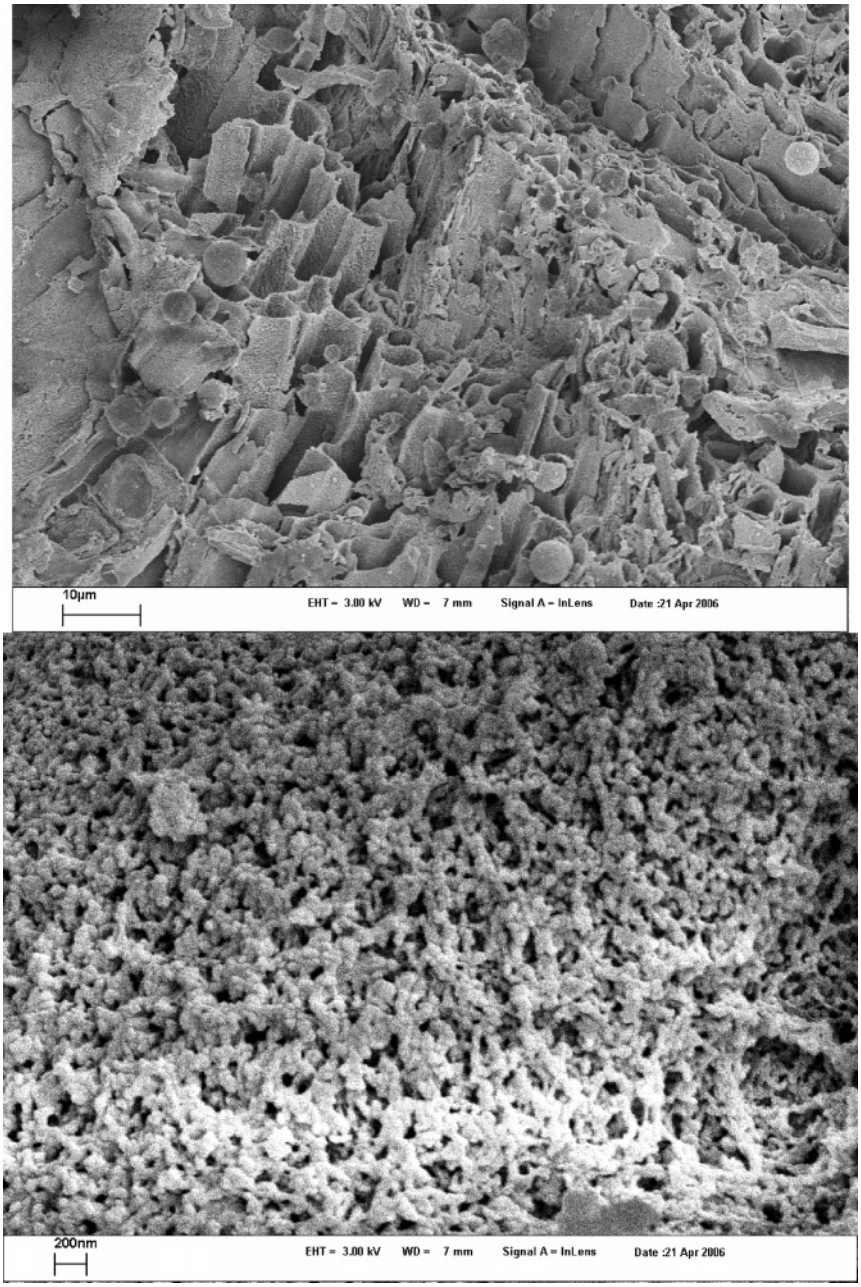

Figure 6. (a) Low-magnification SEM overview of a HTC treated oak leaf; scale bar 10 μm; (b) high-magnification picture (scale bar, 200 nm) of the same sample indicating major changes of the nanostructure and the creation of a mesopore transport system due to chemical dehydration of the scaffold.

"Hard" plant tissue with structural, crystalline cellulose scaffolds (oak leafs, pine cones) showed a different structural disintegration pathway. As the melting point of crystalline cellulose is well above its decomposition temperature, the macro- and microstructure of the biological tissue can be preserved to a large extent in the final carbon material. Figure 6a shows a low magnification of the surface of such a HTC-treated oak leaf. The previous statement is true for carbonization of wood in general, where the preservation of structural detail on the microscale in charcoal is even used to template further ceramic processing (e.g., ref 25).

Obviously, the cellular, layered architecture of the carbohydrate matrix is essentially kept throughout HTC, presumably also supported by the lignin fraction. The soluble carbohydrate components, on the other hand, are transferred in dispersed carbonaceous spheres again, found in the pictures as adhered species. As carbonization of this complex mixture is accompanied with an experimental mass loss of ca. 40 wt % (see Table 1, the theoretical carbonization mass loss for pure glucose is 60 wt %), preservation of outer shape and large-scale structural features on the macro- and mi-

Table 1. Summary of the Experiments Discussed and Some of the Properties of the Resulting Carbons: Samples of Hydrothermal Carbon, Experimental Conditions of Carbonization, and Results of Porosimetry on the Final Carbons

carbon source	mass yield carbon product (dry/dry wt %)	HTC temperature (°C)	mesopore surface area (BET) (m^2/g)	average mesopore size (nm)	carbon content (wt %)
orange peels	37.5	200	0.2	no	68
oak leafs	54.2	200	15.5	28.5	73
pine Cone	63.2	200	34	12	71
pine needles	50.9	200	12	30	71

(25) Greil, P.; Lifka, T.; Kaindl, A. *J. Eur. Ceram. Soc.* **1998**, *18* (14), 1961−1973.

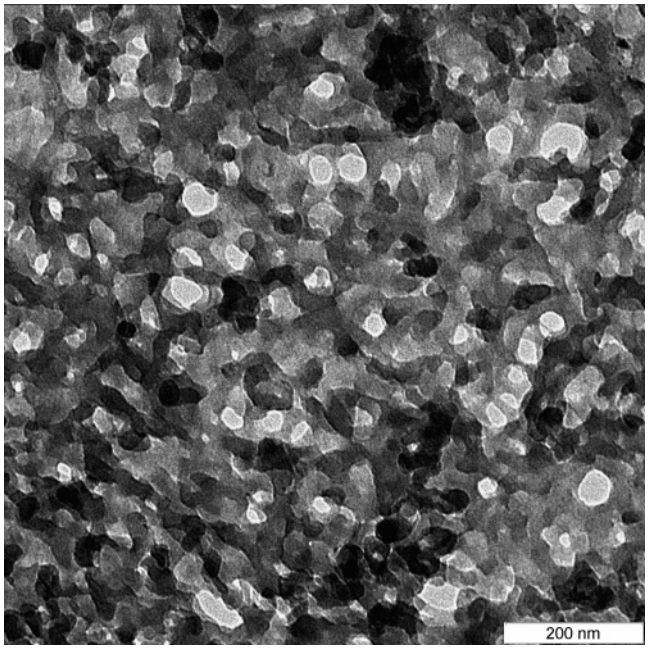

Figure 7. TEM picture of the local structure HTC-treated oak leaves, indicating the complete change of the nanostructure toward a spongelike, cubic porous system with structural elements in the 20−50 nm range.

croscale inevitably has to have consequences on the nanometer scale. Here, HTC treatment changed the structure significantly: the scaffold is rearranged and "opened up" by the hydrothermal dissolution/decomposition reactions. High-resolution SEM (Figure 6b) indicates the presence of a well-developed pore system with apparent pore sizes between 10 and 100 nm. Indeed, removal of 40 wt % water from insoluble carbohydrates leads to materials volume loss or shrinkage, which occurs only on the nanoscale. The same effect is found for the HTC-treated pine cones: on the 100 μm to centimeter scale, the structure is apparently unchanged, except that the cone has lost about 40% of its weight. The HRSEM analysis of the nanostructure proves that removal of the water has again created a continuous nanopore system with structural features very similar to those of Figure 6b (data not shown).

Additional illustrative evidence for the ongoing changes on the nanoscale is given by transmission electron microscopy. Figure 7 depicts a typical, delaminated thin part of the HTC-treated oak leave, indicating the complete chemical reconstitution of the biomass into a spongelike, bicontinuous carbonaceous network with structural elements in the 20−50 nm range. This nicely supports the SEM observations of the surface texture of such carbons. Contrary to the primary biomass and most synthetic polymers, this spongelike structure is stable against the applied high electron fluxes, evidencing the presence of a rather tightly cross-linked carbonaceous material.

The nanometer structure of the pore system was additionally characterized by nitrogen sorption measurements. Figure 8 shows, as an example, the corresponding data of the pine cone carbon. A hysteresis loop in the higher mesopore range is found, indicating the onset of the porous structure at a length scale of about 5 nm. Gas sorption measurements are sensitive only to pore sizes of up to 30 nm, i.e., the macropore structure of the carbons is not reflected in these measurements. Evaluation of the data according to the BJH procedure gave an average pore diameter of the sorption-effective pores of 12 nm and an absolute surface area of 34 m^2/g for only the mesopores. The corresponding measurement on the original dried pine cone material revealed no detectable porosity at all.

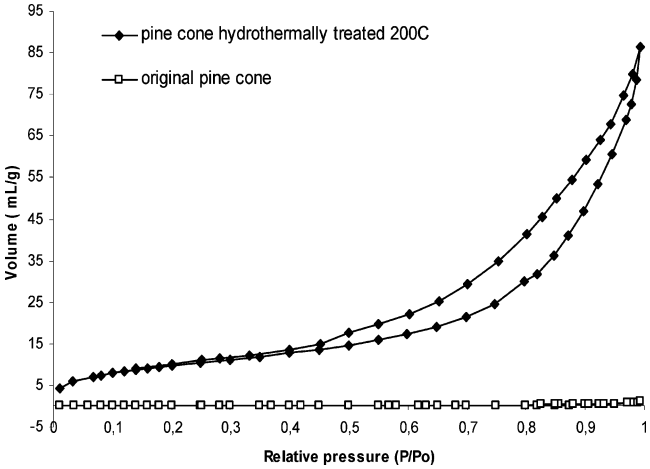

Figure 8. Gas sorption measurements characterizing the mesopore structure of the as-synthesized hydrothermal carbons.

All the other synthesized HTC samples showed, with minor differences, similar gas sorption behaviors, which is due to either a similar spongelike pore system or the corresponding interstitial pore system between the aggregated carbon nanospheres. It must be mentioned that all the samples contain practically no micropores (<2 nm diameter). This is different from standard activated carbons made by high-temperature processes, which have a much higher specific surface area but are practically exclusively based on micropores (below 2 nm pore size).[26]

Again, the surface chemistry of the nanoporous carbons turned out to be very hydrophilic, as indicated by water sorption experiments (data not shown), but the spontaneous uptake of water in these structures is on the macroscopic scale. We attribute this interesting surface chemistry again to the presence of polar groups, which are immobilized throughout HTC at the biocarbon/water interface.

Conclusion and Outlook

Complex waste biomass was hydrothermally transformed under rather mild conditions (200 °C for 16 h) to carbonaceous structures, which are chemically and spectroscopically similar to peat or lignite, depending on the time and temperature. Contrary to simple expectations, the presence of other components in the plant material does not hinder the reaction, but leads to the development of useful nanostructures, instead.

For soft biomass, we found hydrophilic and water-dispersible carbonaceous nanoparticles in the size range of 20−200 nm, coexisting with some larger structures. The occurrence as spherical particles indicates that the soft biomass is first liquefied, and then carbonized, which offers additional possibilities to chemically interfere with this

(26) Kaneko, K.; Ishii, C.; Ruike, M.; Kuwabara, H. *Carbon* **1992**, *30* (7), 1075−1088.

complex process. Such carbon nanoparticles might represent an alternative for current carbon blacks made by (much less sustainable) flame processes, but because of the excellent price base might also end up in novel materials applications, such as carbon reinforced concrete.

For hard biomass, an "inverted" structure was found, with the carbon being the continuous phase, that was perforated by a spongelike, continuous system of nanopores. Also, because of the remainder of ca. 20 wt % functional groups and oxygen, these products are hydrophilic and can be easily wetted with water. This is ideal for water binding and capillarity. By simple chemical means, the product is practically indistinguishable from a high-value mesoporous sorption carbon.

HTC is therefore an alternative and simple option to use wet, low-value biomass, leading to hard carbonaceous products, with the majority of original carbon being sequestered in the solid. A key feature is not only the occurrence of carbonization in itself but also the appearance as useful nanostructures with an appropriate surface chemistry. To analyze the potential value for a real application on larger scales, we necessarily have to explore engineering aspects. This should be quite similar to the more demanding process of hydrothermal gasification of wet biomass in near supercritical water, which already has reached impressive sophistication and performance.[18,27] From the viewpoint of chemistry, the clarification of the molecular mechanisms of dehydration and a more careful look onto the liquid intermediates is appealing, as it potentially allows a more controlled approach to the variation of the resulting structures and their surface chemistry.

Acknowledgment. This work was supported by the Project House "ENERCHEM" of the Max Planck Society, the Chinese−German Partner group program of the MPG, and the Centurial Program of the Chinese Academy of Sciences and the NSFC.

CM0707408

(27) Matsumura, Y.; Minowa, T.; Potic, B.; Kersten, S. R. A.; Prins, W.; van Swaaij, W. P. M.; van de Beld, B.; Elliott, D. C.; Neuenschwander, G. G.; Kruse, A.; Antal, M. J. *Biomass Bioenergy* **2005**, *29* (4), 269−292.